

Tensile Properties, Water Resistance, and Thermal Properties of Linear Low-Density Polyethylene/Polyvinyl Alcohol/Kenaf Composites: Effect of 3-(trimethoxysilyl)propyl Methacrylate (TMS) as a Silane Coupling Agent

Ai Ling Pang,^a Hanafi Ismail,^{a,b,*} and A. Abu Bakar^a

Composites containing linear low-density polyethylene/polyvinyl alcohol and various loadings of kenaf fiber were prepared using a Haake internal mixer. The loading of kenaf fiber varied from 10 to 40 parts per hundred resin (phr). The coupling agent 3-(trimethoxysilyl)propyl methacrylate (TMS) was evaluated for its effect on the processing torque, tensile properties, morphology, water resistance, and thermal properties of the composites. Composites without TMS were used as the control. The composites made from TMS-treated kenaf yielded higher stabilization torque, tensile strength, tensile modulus, water resistance, and thermal properties than the control composites. The improvements were attributed to the coupling effect of TMS.

Keywords: Linear low-density polyethylene; Polyvinyl alcohol; Kenaf composites; Silane methacrylate

Contact information: a: School of Materials and Mineral Resources Engineering and b: Cluster for Polymer Composites (CPC), Science and Engineering Research Centre (SERC), Universiti Sains Malaysia (USM), Engineering Campus, 14300 Nibong Tebal, Penang, Malaysia;

* Corresponding author: ihanafi@usm.my

INTRODUCTION

The introduction of various types of natural fibers into polymer matrices has been widely explored over the last few decades (Malkapuram *et al.* 2009). Increasing interest in the use of natural fibers comes from their relatively low cost, biodegradability, and availability (Akil *et al.* 2011; Pua *et al.* 2013), resulting in products that are cost-effective and environmentally friendly. Kenaf (*Hibiscus cannabinus* L.) fiber is frequently used in polymer composites (Ismail *et al.* 2010; Rohani *et al.* 2010; Pang and Ismail 2014; Saba *et al.* 2015). Kenaf absorbs nitrogen and phosphorus in soil, and it absorbs carbon dioxide at a high rate (Akil *et al.* 2011; Nurfatimah *et al.* 2014). In addition, kenaf is known for its good mechanical properties and fatigue and corrosion resistance (Maizatul *et al.* 2013). In Malaysia, kenaf plantations produce large quantities of biomass because of its wide usage in various applications, such as food packaging, furniture, sports and leisure, and automotive components (Meon *et al.* 2012).

The incorporation of kenaf fiber in polymer composites provides several advantages; however, a major drawback is the potential incompatibility between the kenaf and the polymer. Generally, polymers are hydrophobic and incompatible with hydrophilic natural fibers. The poor compatibility between kenaf fibers and polymer systems may yield composites with poor properties. In addition, the highly hydrophilic nature of natural fibers often causes high moisture absorption in the polymer composites (Ismail *et al.* 2010;

Noranizan and Ahmad, 2012; Tan *et al.* 2014). Consequently, the dimensions of the composite may change the resulting properties.

Chemical modifications improve the interactions at the interface between natural fibers and the polymer matrix (Ismail *et al.* 2010). Many different chemical modifications of natural fiber/polymer composites have been studied (Malkapuram *et al.* 2009; Pang and Ismail 2014).

To date, 3-(trimethoxysilyl)propyl methacrylate (TMS) was not yet been used as coupling agent in the linear low-density polyethylene/polyvinyl alcohol/kenaf composites. TMS was chosen as coupling agent to enhance the interfacial adhesion between kenaf and linear low-density polyethylene/polyvinyl alcohol matrices. In this study, the effects of 3-(trimethoxysilyl)propyl methacrylate (TMS) on the processing, tensile properties, water resistance, and thermal properties of composites were investigated.

EXPERIMENTAL

Materials

Linear low-density polyethylene (LLDPE) was supplied by the PT Lotte Chemical Titan Nusantara, Indonesia, with a melt flow rate of 1 g/10 min at 190 °C and a density of 0.92 g/cm³. Poly(vinyl alcohol) (PVA) (> 99% hydrolyzed) was supplied by Sigma-Aldrich Sdn. Bhd., Malaysia, with a molecular weight of 89,000 to 98,000 g/mol and a density of 1.269 g/cm³. Three-(trimethoxysilyl)propyl methacrylate (TMS) was supplied by Sigma-Aldrich Sdn. Bhd., Malaysia, with a molecular weight of 248.35 g/mol. Kenaf (KNF) was obtained from the National Kenaf and Tobacco Board (LKTN), Kelantan, Malaysia. Before treatment, the KNF was processed in a mini grinder from the Rong Tsong Precision Technology Co., Taiwan (Product Id: RT-34), to yield KNF powder with an average particle size of 75 µm.

Treatment of KNF by TMS

The untreated KNF was used as the control in this study, and the preparation of the TMS-treated KNF was as follows. First, 5.0 (wt.%) of 3-(trimethoxysilyl)propyl methacrylate (weight percentage compared to KNF) was dissolved for hydrolysis in a mixture of a 3:2 ratio of ethanol and water. KNF was added to the mixture, and the solution was maintained at pH 4 with acetic acid. The mixture was stirred continuously for 1 h. Then, the KNF was soaked in the solution for 3 h, washed with distilled water, and oven-dried at 60 °C overnight.

Composite preparation

The KNF was dried in a vacuum oven at 80 °C for 24 h before preparation of the composite. The weight ratio of LLDPE/PVA was maintained at 60:40 (wt.%), as this ratio gives the best overall blend properties (Ismail *et al.* 2009). The melt compounding of LLDPE/PVA/KNF composites with TMS was done in an internal mixer (Model R600/610, Thermo Haake Polydrive, Germany) at a temperature of 150 °C and a rotor speed of 50 rpm. The LLDPE was loaded into the mixing chamber and allowed to melt for 2 min, followed by the addition of PVA and TMS-treated KNF after 2 and 6 min, respectively. The processing torque was recorded for each sample. The compounded samples were then compression-moulded at 150 °C into 1-mm thick sheets using an electrically-heated hydraulic press (Model KT-7014 A, GoTech Testing Machine, Taiwan).

Table 1. Formulation of Control and 3-(Trimethoxysilyl)propyl Methacrylate (TMS)-Treated Composites

Materials	Control	TMS-treated
LLDPE/PVA	60:40	60:40
KNF (phr)	0,10,20,30,40	10,20,30,40
TMS (wt.%)	-	5

Methods

Measurement of tensile properties

The tensile testing was done in accordance with the ASTM D638-10 (2010) standard using an Instron 3366 Universal Testing Machine (Norwood, MA, USA). The crosshead speed was set at 5 mm/min, with a constant gauge length of 50 mm. The tests were performed at 25 ± 3 °C on the 1-mm thick, dumbbell-shaped specimens, and an average of five readings of tensile strength, tensile modulus, and elongation at break were recorded.

Morphological study

A Carl Zeiss Supra-35VP field emission scanning electron microscope (FESEM; Carl Zeiss Microscopy GmbH, Jena, Germany) was used to observe the tensile-fractured surfaces of the specimens. The fractured surfaces of the specimens were sputter-coated with a thin layer of gold to avoid electrostatic charging and poor resolution. The specimens were then mounted onto aluminum stubs for examination.

Water absorption

The water uptake test was carried out in accordance with the ASTM D570-098 testing standard (2010). The specimens were first dried in an oven for 24 h at 50 °C until a constant weight was obtained. The weight difference after immersion was recorded by weighing them periodically on a Sartorius balance (BS224S, Gottingen, Germany), with a precision of 1 mg. The excess water on the specimen surfaces was removed with tissue paper before weighing. The water uptake test was performed for 30 days, and the percentage of water uptake was calculated using Eq. 1,

$$W_t(\%) = \frac{W_2 - W_1}{W_1} \times 100 \quad (1)$$

where W_t is the total water uptake by the specimen, and W_1 and W_2 are the weights of the specimen before and after immersion in distilled water, respectively.

Thermogravimetric analysis (TGA)

Thermogravimetric analysis (TGA) was performed using a Pyris 6 thermogravimetric analyzer (Perkin Elmer, Waltham, MA, USA). Thermogravimetric analysis was conducted in the ramp mode from 30 to 600 °C, under a nitrogen flow rate of 50 mL/min. The heating rate was 20 °C/min.

Fourier transform infrared (FTIR) spectroscopy

The functional groups and chemical characteristics of the control and TMS-treated LLDPE/PVA/KNF composites were obtained using a Perkin Elmer System 2000 FTIR spectrometer (Waltham, MA, USA). The spectrum resolution was 4 cm^{-1} in a spectral range of 4000 to 550 cm^{-1} .

RESULTS AND DISCUSSION

Processing Torque

Processing torque-time curves can be used to evaluate the melt processing characteristics of composites (Sarifuddin *et al.* 2013). Figure 1 illustrates the processing torque of the LLDPE/PVA/KNF composites with TMS at different KNF loadings. The torque value increased drastically at each time period when LLDPE, PVA, and TMS-treated KNF were incorporated into the mixing chamber. This behavior was a consequence of the resistance of each material to flow in the mixing chamber. The torque lessened and stabilized at the end of mixing (10 min), indicating that LLDPE and PVA were completely melted. However, composites with higher TMS-treated KNF loadings, *i.e.*, 40 phr, yielded higher processing torque values at the end of mixing. This can be ascribed to an enhanced interfacial adhesion between KNF and LLDPE/PVA in the presence of TMS.

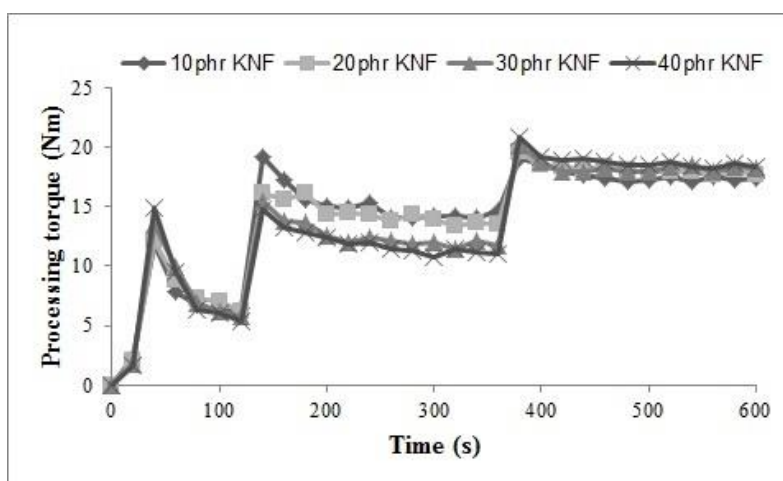


Fig. 1. Effect of 3-(trimethoxysilyl)propyl methacrylate (TMS) on processing torque of LLDPE/PVA/KNF composites at different KNF loadings

Figure 2 illustrates the stabilization torque of control and TMS-treated LLDPE/KNF/PVA composites at different KNF loadings.

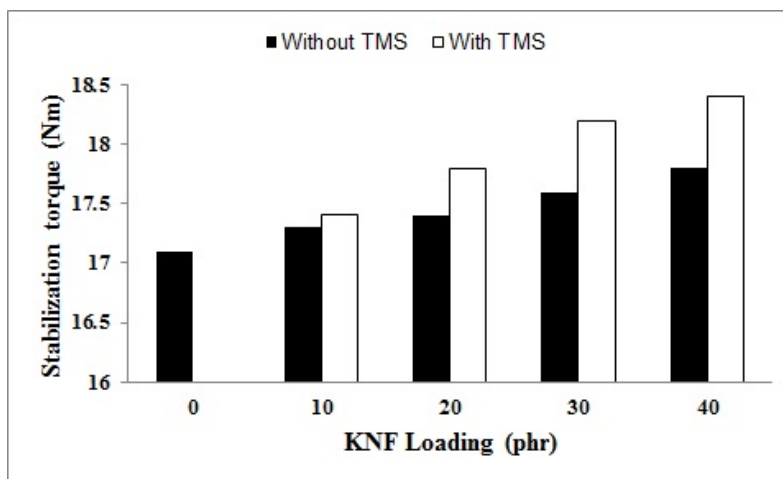


Fig. 2. Effect of TMS on the stabilization torque of LLDPE/PVA/KNF composites at different KNF loadings

The stabilization torque is the equilibrium torque value that was recorded at the end of the mixing, *i.e.*, at the end of 10 min. The stabilization torque increased for both composites as the KNF loading increased, which suggested that the processing of the composites is easier at lower KNF loadings (Pang *et al.* 2015). However, at similar KNF loadings, composites with TMS exhibited higher stabilization torque values compared with the control composites. This finding was attributed to enhanced interfacial interactions between KNF and the LLDPE/PVA matrix, which is explained in more detail below.

Tensile Properties

Figure 3 shows the tensile strength of control and TMS-treated LLDPE/KNF/PVA composites at different KNF loadings. The addition of KNF reduced the tensile strength of both composites. This observation suggests an incompatibility between the hydrophilic KNF and the hydrophobic LLDPE, in addition to the hydrophobic LLDPE and hydrophilic PVA matrix itself. As a result, a weak interfacial adhesion formed between the KNF and LLDPE/PVA, as well as the LLDPE and PVA. Therefore, when stress was applied during tensile testing, the poor stress transfer between the fiber-matrix resulted in poor tensile properties. When the fiber content was increased, the area of weak interfacial also increased (Chun *et al.* 2013). Therefore, as the KNF loading increased, the tensile strength decreased for both composites. A previous study by Pang and Ismail (2013) found a similar trend in the tensile strength of kenaf-filled polypropylene/waste pulverized tire composites. However, at similar KNF loadings, the composites with TMS exhibited higher tensile strengths than composites without TMS. This effect was attributed to the coupling effect of TMS, which enhanced interfacial interactions between KNF and the LLDPE/PVA matrix. TMS promoted better interfacial adhesion between KNF and LLDPE/PVA matrix, which was also seen in FESEM micrographs (Fig. 9b and 10b).

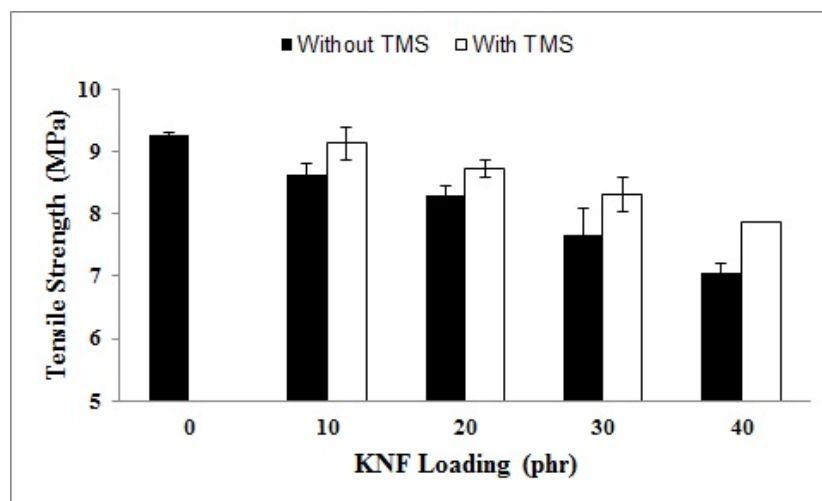


Fig. 3. Effect of TMS on the tensile strength of LLDPE/PVA/KNF composites at different KNF loadings

The possible coupling effect of TMS in LLDPE/PVA/KNF composites can be explained in several steps (Figs. 4 to 7). The first step is the hydrolysis of TMS (silane coupling agent) to form silanol (Fig. 4), followed by the reaction of silanol with the hydroxyl groups of KNF to form an intermediate 1 (Fig. 5).

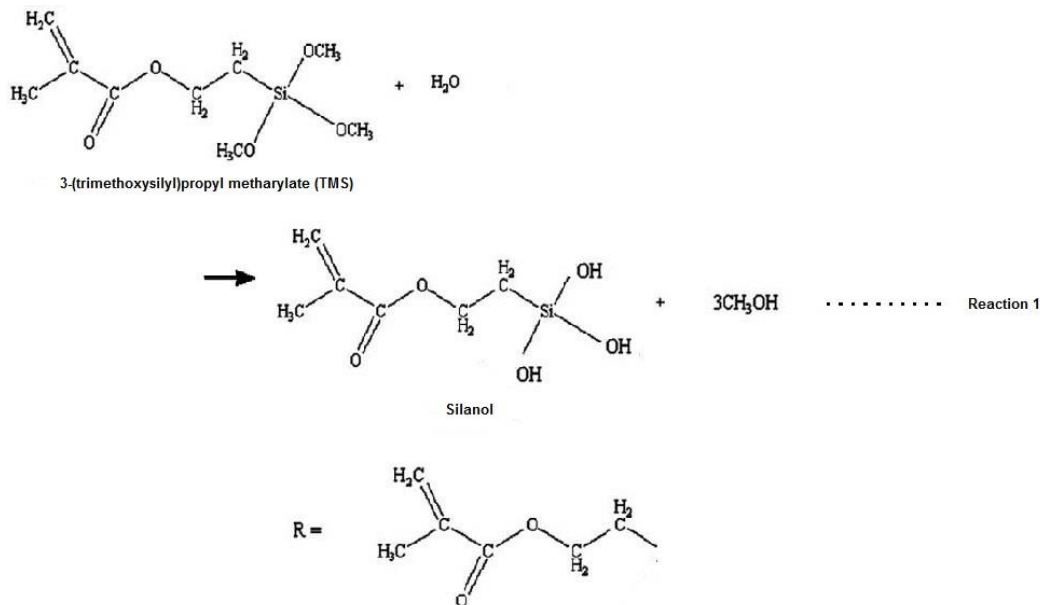


Fig. 4. Hydrolysis of TMS (Re-drawn from Nordin *et al.* 2012; Eng *et al.* 2014)

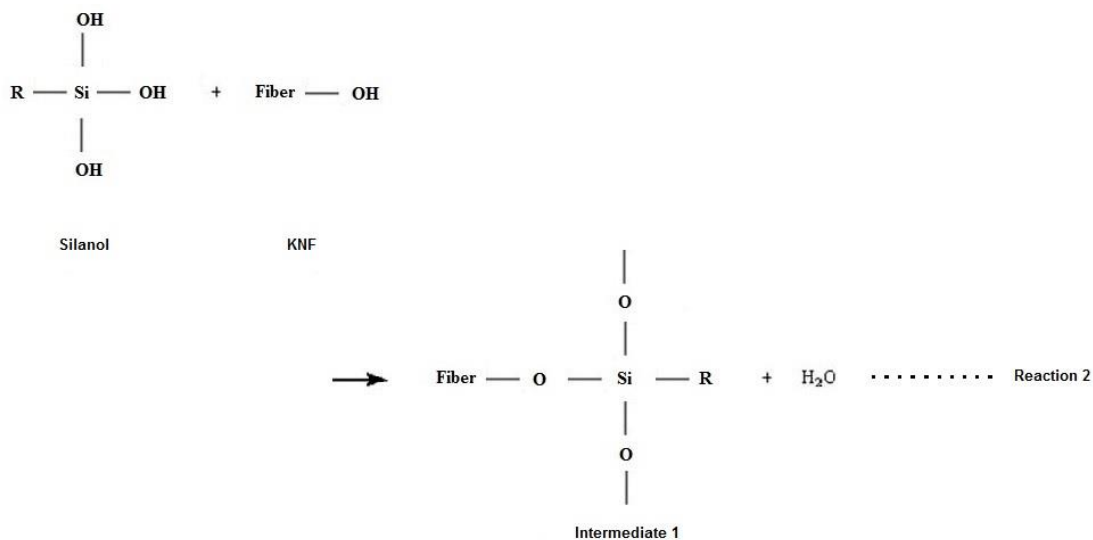


Fig. 5. Proposed interaction between the TMS coupling agent and KNF

The TMS-treated KNF (intermediate 1) then will react with the PVA and forming another intermediate 2 (Fig. 6). The hydroxyl group of PVA may react with the silanol group in intermediate 1, forming a Si-O-C bonding as shown in Fig. 6. Next, a reaction occurs between the hydrophobic portion of intermediate 2 and the LLDPE, as shown in Fig. 7.

Because of their similar hydrophobicity, the hydrophobic group (R = C₆H₈O₂~) in intermediates 2 is attracted to the hydrophobic LLDPE. The interface between the KNF and the LLDPE/PVA was likely enhanced by the presence of TMS. Therefore, TMS is found to be effective as a coupling agent for this LLDPE/PVA/KNF composite.

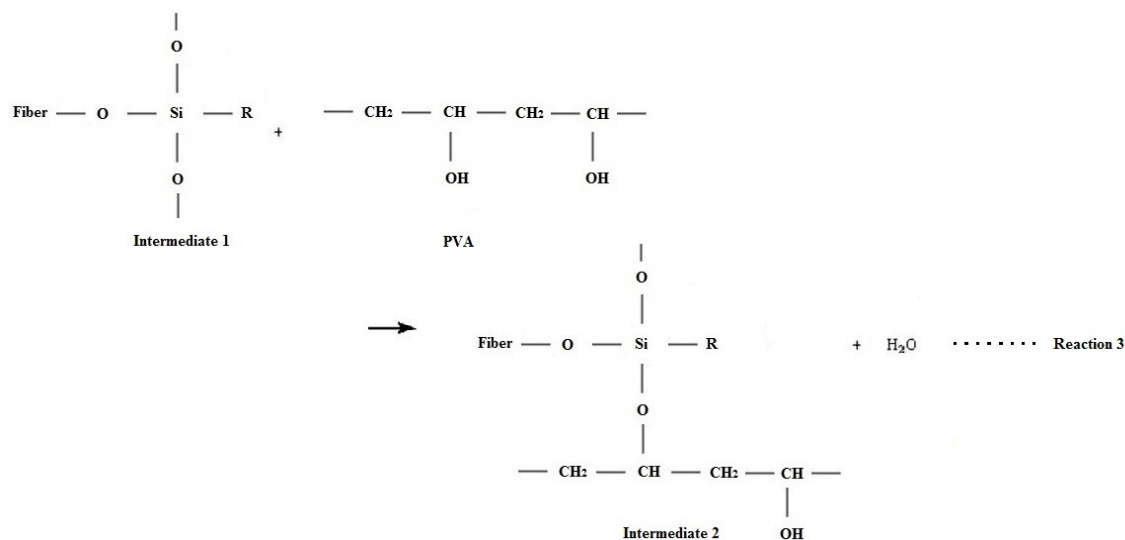


Fig. 6. Proposed interaction between the TMS-treated KNF (Intermediate 1) and PVA

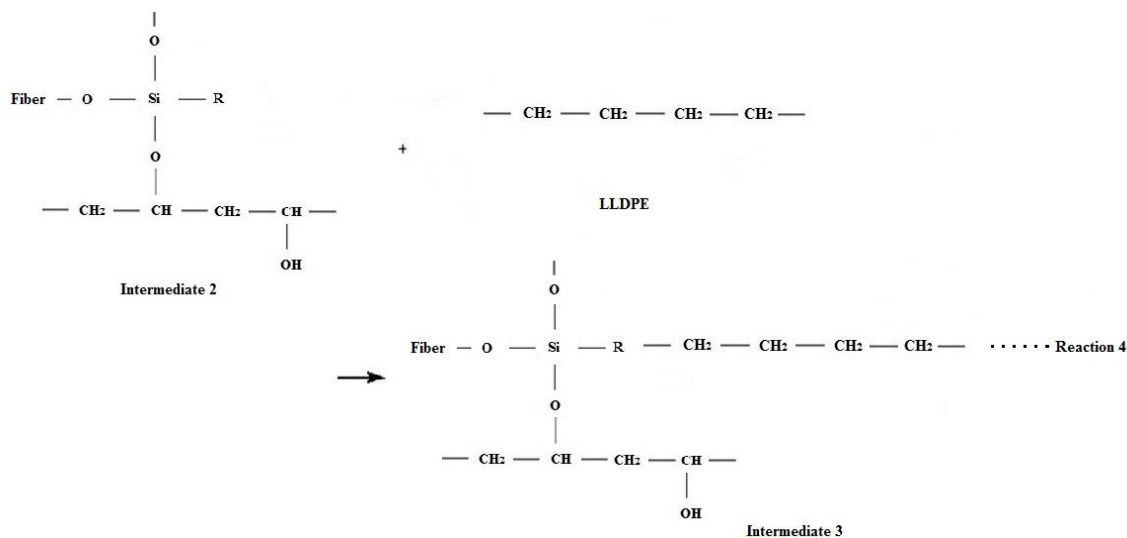


Fig. 7. Proposed interaction between the Intermediate 2 and LLDPE

Figure 8 shows the tensile modulus of the control and TMS-treated LLDPE/KNF/PVA composites at different KNF loadings. The addition of KNF increased the stiffness of both composites. Generally, the filler has a higher stiffness than the matrix, which increases the modulus of the composites (Faisal *et al.* 2010; Sarifuddin *et al.* 2013). When the KNF loading increased, the stiffening effect of KNF on the composite also increased. Thus, the tensile modulus increased with increasing KNF loading for both composites. However, at similar KNF loadings, the tensile modulus of the composites with TMS was higher compared to composites without TMS. This result suggested that the stiffness of the composites was enhanced by the TMS treatment. In addition, the presence of TMS promoted better fiber-matrix interfacial interactions, also contributing to the higher tensile modulus. According to Eng *et al.* (2014), the tensile modulus of methacrylate silane-treated oil palm mesocarp/polylactic acid/polycaprolactone/nanoclay biocomposites was higher than untreated composites.

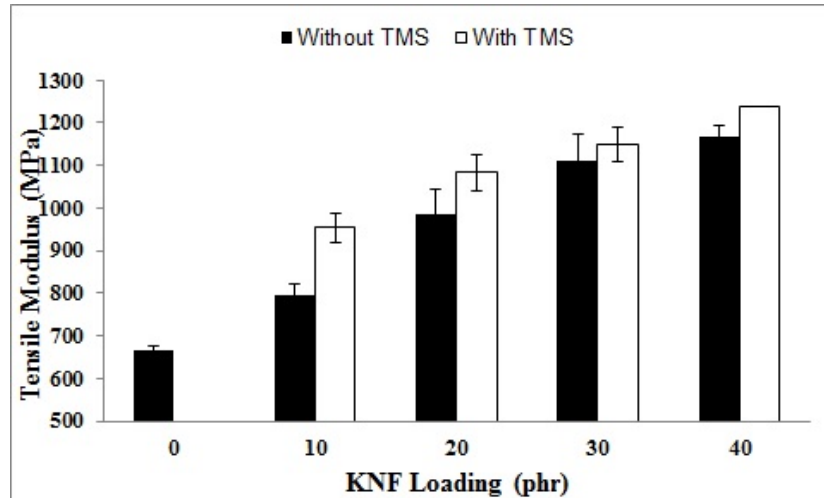


Fig. 8. Effect of TMS on the tensile modulus of LLDPE/PVA/KNF composites at different KNF loadings

Figure 9 shows the elongation at break of control and TMS-treated LLDPE/KNF/PVA composites at different KNF loadings. The elongation at break decreased for both composites with increasing KNF loading. This is a common trend because the addition of filler restricts the polymer chain mobility (Santiago *et al.* 2011; Chun *et al.* 2013). At similar KNF loadings, the elongation at break of the composites with TMS was lower than composites without TMS. This is because the TMS treatment on KNF has leads to the enhancement in the interfacial adhesion between KNF and LLDPE/PVA. Consequently, the ductility of the composites was reduced by the interfacial adhesion enhancement.

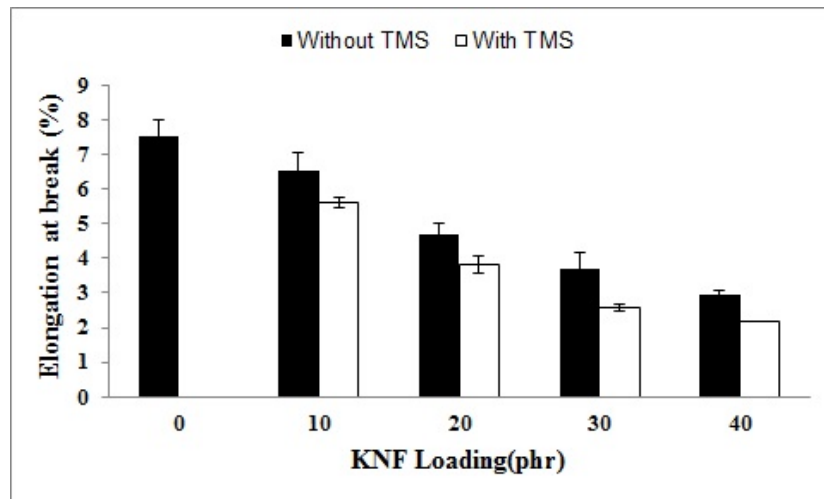


Fig. 9. Effect of TMS on the elongation at break of LLDPE/PVA/KNF composites at different KNF loadings

Morphological Study

The morphology of the tensile fractured surfaces of control and TMS-treated LLDPE/PVA/KNF composites at 10 phr and 40 phr KNF loadings are shown in Figs. 10

and 11, respectively. Figure 10(a) shows that KNF was loosely embedded in the LLDPE/PVA matrix to form fiber agglomerates. Figure 11(a) shows the presence of fiber agglomerates and fiber pull-out, which was more obvious at higher KNF loadings. This observation implies poor interfacial adhesion between the KNF and the LLDPE/PVA matrix, which lead to lower tensile properties. In contrast, Figs. 10(b) and 11(b) show that composites with TMS resulted in improved interfacial adhesion, as recognized by the tight adherence of KNF to the LLDPE/PVA matrix, with no gaps between them. In addition, no fiber debonding was observed for composites with TMS. This result confirmed the improvement in the tensile properties of composites with TMS. Hence, TMS was an effective coupling agent for the LLDPE/PVA/KNF composites.

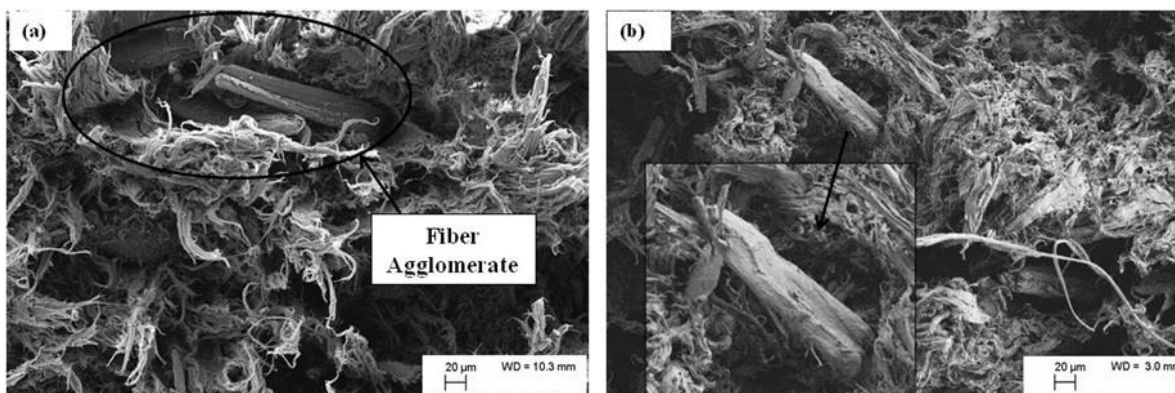


Fig. 10. Scanning electron micrographs of the tensile-fractured surfaces of the (a) control and (b) TMS-treated LLDPE/PVA/10KNF composites at a magnification of 200X

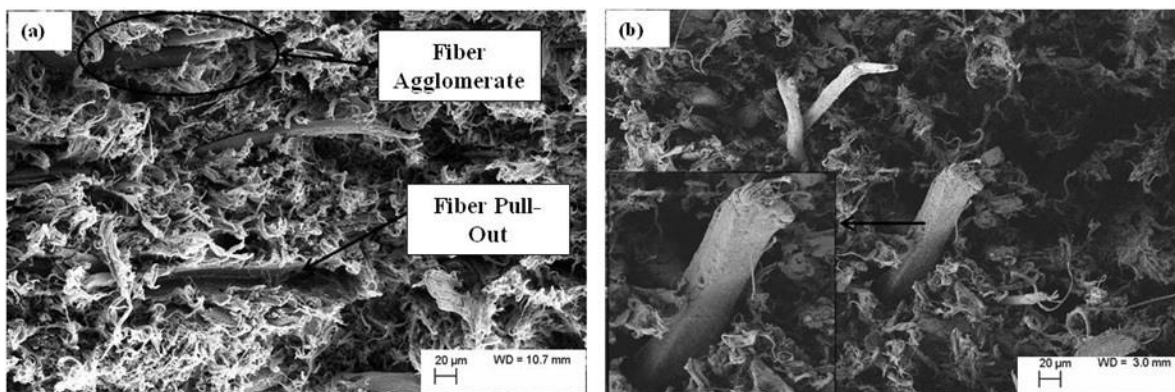


Fig. 11. Scanning electron micrographs of the tensile-fractured surfaces of the (a) control and (b) TMS-treated LLDPE/PVA/40KNF composites at a magnification of 200X

Fourier Transform Infrared Spectroscopy

FTIR spectra of the control and TMS-treated LLDPE/PVA/10-KNF composites are shown in Fig. 12. Both control and composites with TMS showed characteristic peaks within the range 3200 to 3400 cm^{-1} (hydroxyl group (O-H) stretching), peaks within the range of 2900 to 2700 cm^{-1} (CH_2 and CH bending), peaks within the range 1600 to 1645 cm^{-1} (adsorbed water in cellulose or carboxyl/ester groups ($\text{C}=\text{O}$) of hemicellulose), and peaks within the range 1460 to 1465 cm^{-1} (CH_2 bending) (Majid *et al.* 2010; Pang and Ismail 2013; Pua *et al.* 2013; Eng *et al.* 2014). However, the spectrum of TMS-treated composites showed a decreased intensity at peak range of 3200 to 3400 cm^{-1} . This

observation might be due to the occurrence of hydrogen bonding formation after TMS treatment. This result showed there is a reaction between the hydroxyl groups of KNF and the alkoxy functional groups of TMS. Majid *et al.* (2010) has reported the similar findings in the compatibilization of LDPE/TPSS-kenaf fiber composites using PE-g-MA compatibilizer.

The spectra of both the control composites and TMS-treated composites displayed a strong peak around 1750 cm^{-1} , which corresponded to carbonyl stretching ($\text{C}=\text{O}$) (Rangel-Vazquez and Leal-Garcia 2010; Eng *et al.* 2014). The carbonyl peaks are 1745 cm^{-1} and 1750 cm^{-1} for control composites and TMS-treated composites, respectively. This result clearly shows there is a carbonyl stretching peak shifting in the TMS-treated composites.

According to Eng *et al.* (2014), when there is an interaction in the polymer composites, shifting of peaks in IR spectra may occur. Meanwhile, Majid *et al.* (2010) claimed that polymer composites with good compatibility will result in greater correlative peak shift and change in peak shapes. Thus, it is indicated that there is some physical interactions occurred between the methacrylate reactive groups of TMS on surface of KNF with LLDPE/PVA matrix.

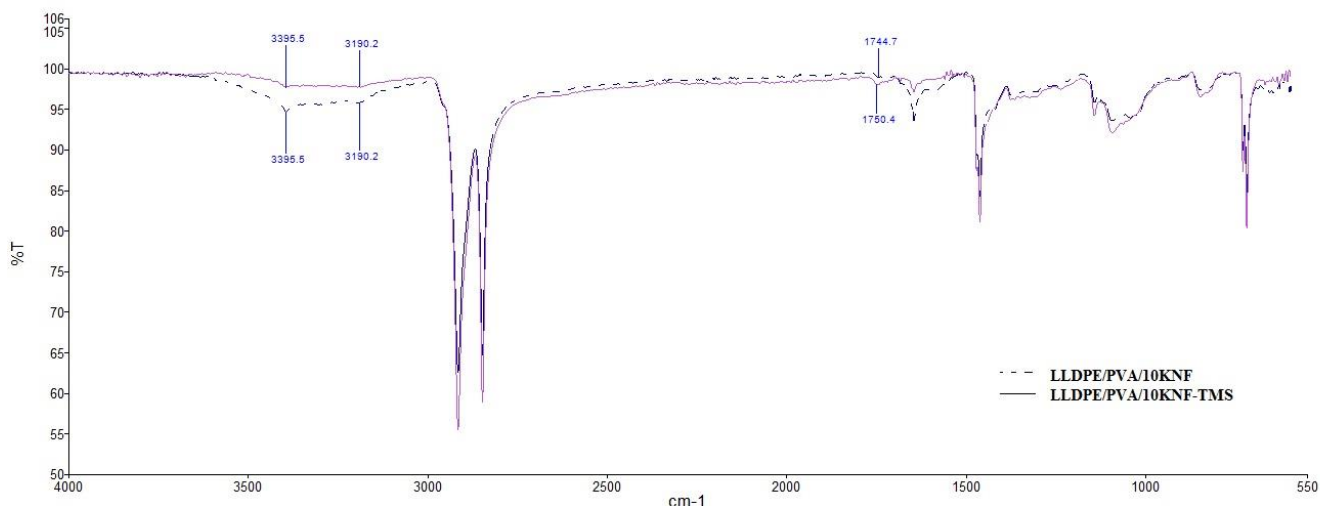


Fig. 12. Fourier transform infrared spectra of the control and TMS-treated LLDPE/PVA/10-KNF composites

Water Retention

Figure 13 shows the water absorption of control and TMS-treated LLDPE/KNF/PVA composites at different KNF loadings after approximately 35 days. The water absorption increased with increasing KNF loading for both composites. The water absorption of cellulose fiber composites resulted from the formation of hydrogen bonds between hydroxyl groups of cellulose and water molecules (Demir *et al.* 2006). Majid *et al.* (2010) found that the water absorption of LDPE/TPSS-kenaf fiber composites was a consequence of the hydrophilic nature of both kenaf fiber and starch. In the present study, water absorption by the composites was attributed to both KNF and PVA. According to Tan *et al.* (2014), the water absorption ability of kenaf-polyvinyl alcohol (PVOH) composites comes from both kenaf and PVOH.

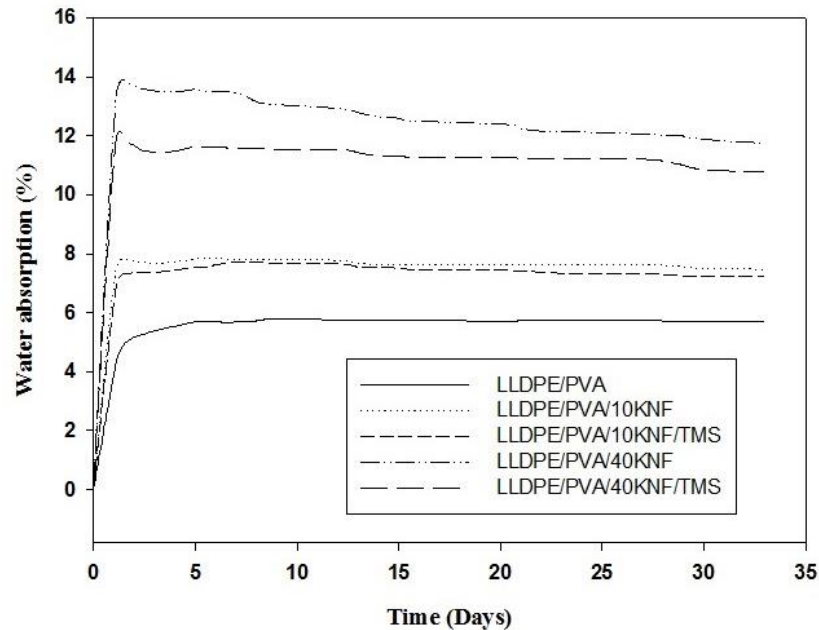


Fig. 13. Effect of TMS on the water absorption of LLDPE/PVA/KNF composites

Figure 14 shows that the water absorption percentage at the equilibrium stage of the composites with TMS was lower than the control composites. The lower equilibrium water absorption of TMS-treated composites was a result of hydrogen bonding between TMS and the hydroxyl groups of KNF. Therefore, the water absorption by the TMS-treated composites was restricted. Osman *et al.* (2012) reported a similar finding on the water absorption of silane and maleic anhydride-grafted polypropylene (MAPP)-treated recycled newspaper-filled polypropylene/natural rubber composites. Another reason for the lower water absorption was the improved fiber-matrix interfacial adhesion after the TMS treatment. However, an increase in the equilibrium water absorption with KNF loading was expected for both composites. This is because of the increase in the volume of the interfacial region, resulting in greater penetration of water molecules into the composites (Osman *et al.* 2012).

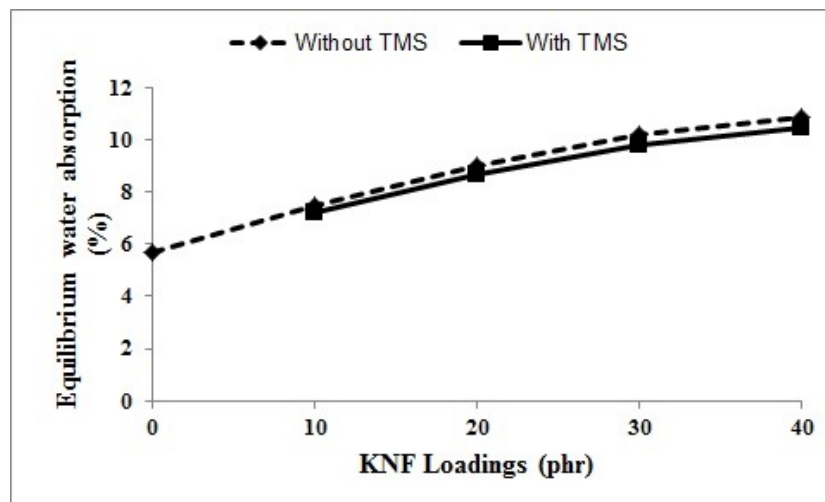


Fig. 14. Effect of TMS on the equilibrium water absorption of LLDPE/PVA/KNF composites

Thermogravimetric Analysis (TGA)

Figures 15 and 16 show the TGA and DTG curves of control and TMS-treated LLDPE/PVA/KNF composites at 10 phr and 40 phr KNF loadings. According to the TGA curves in Fig. 15, the thermal degradation of both composites occurred in three steps, which was confirmed by the presence of three peaks in the DTG curves (Fig. 16). The three steps of thermal degradation involved: i) evaporation of absorbed moisture on the surface of the composites at 100 °C (Pang *et al.* 2015), ii) decomposition of hemicelluloses, cellulose, and lignin at 200 to 400 °C (Fisher *et al.* 2002; Chun *et al.* 2013), and iii) decomposition of the LLDPE/PVA matrix at 450 to 550 °C.

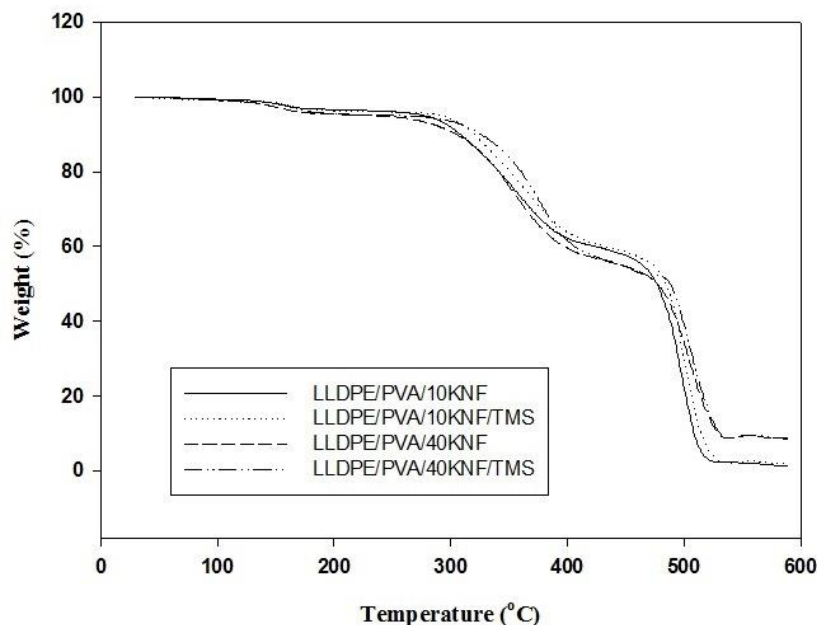


Fig. 15. TGA curves of control and TMS-treated LLDPE/PVA/KNF composites at different KNF loadings

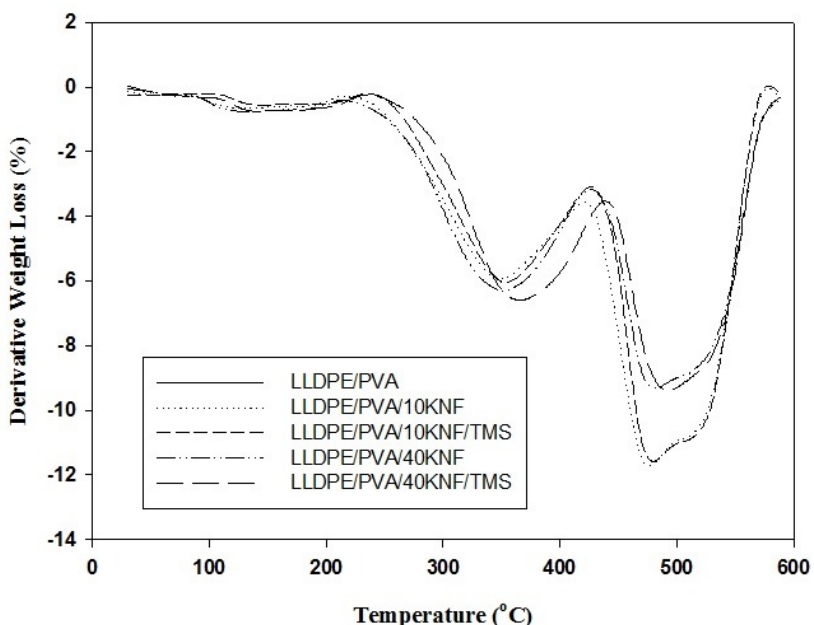


Fig. 16. DTG curves of control and TMS-treated LLDPE/PVA/KNF composites at different KNF loadings

Table 2 shows the TGA parameters of control and TMS-treated LLDPE/PVA/KNF composites. The $T_{5\%}$ and $T_{50\%}$ values represent the degradation at 5% and 50% sample weight loss, respectively. The $T_{5\%}$ of both composites with and without TMS decreased with increasing KNF loading, suggesting that the early thermal degradation of the composites was a result of their thermally instable KNF. However, at similar KNF loadings, the $T_{5\%}$ of the composites with TMS was higher than composites without TMS. This result was attributed to improvement in the interfacial interaction between KNF and the LLDPE/PVA matrix. Hence, higher temperature was required to initiate early degradation of the composites. From Table 2, the $T_{50\%}$ and char residue percentage of TMS-treated composites were higher than control composites. These results implied that the addition of TMS increased the thermal stability of the composites to some extent. Composites with TMS required higher temperature to initiate thermal degradation, forming more char residue, which acted as a thermal protective layer and slowed the decomposition of the composites. The char residue forms a layer between the polymeric material and the heat source, which slows degradation (Beyler and Hirschler 2001). Thus, TMS-treated composites were more thermally stable than the controls.

Table 2. TGA Parameters of Control and TMS-Treated LLDPE/PVA/KNF Composites

Sample	$T_{5\%}$ (°C)		$T_{50\%}$ (°C)		Char Residue (%)	
	Control	TMS-treated	Control	TMS-treated	Control	TMS-treated
LLDPE/PVA	283		473		0.762	
LLDPE/PVA/10-KNF	277	292	476	483	1.308	1.992
LLDPE/PVA/40-KNF	234	257	484	486	8.560	8.720

$T_{5\%}$: temperature at 5% weight loss; $T_{50\%}$: temperature at 50% weight loss

CONCLUSIONS

1. The addition of 3-(trimethoxysilyl)propyl methacrylate (TMS) successfully enhanced the tensile strength, tensile modulus, water resistance, and thermal stability of LLDPE/PVA/KNF composites.
2. FESEM micrographs showed that KNF strongly adhered to the LLDPE/PVA matrix in the presence of TMS, indicating that TMS improved the interfacial adhesion between KNF and the LLDPE/PVA matrix.
3. FTIR spectra showed that the intensity of the hydroxyl group stretching was reduced, and the formation of strong carbonyl stretching indicated an interaction between KNF and the LLDPE/PVA matrix in the presence of TMS.

ACKNOWLEDGMENTS

The authors express their appreciation to the National Kenaf and Tobacco Board (LKTN), Kelantan, Malaysia, for supplying the KNF fiber, the RUC research grant (1001/PKT/8640014) from the Universiti Sains Malaysia, and MyBrain15 for their sponsorship.

REFERENCES CITED

- Akil, H. M., Omar, M. F., Mazuki, A. A. M., Safiee, S., Ishak, Z. A. M., and Abu Bakar, A. (2011). "Kenaf fiber reinforced composites: A review," *Mater Des.* 32(8-9), 4107-4121. DOI: 10.1016/j.matdes.2011.04.008
- ASTM D570-098. (2010). "Standard test method for water absorption of plastics," ASTM International, West Conshohocken, USA.
- ASTM D638-10 (2010). "Standard test method for tensile properties of plastics," ASTM International, West Conshohocken, USA.
- Beyler, C. L., and Hirschler, M. M. (2001). "Thermal decomposition of polymers," in: *SFPE Handbook of Fire Protection Engineering* (3rd ed.), P. J. DiNenno (Ed.), National Fire Protection Association, Quincy, MA, USA, Chapter 7.
- Chun, K. S., Husseinsyah, S., and Azizi, F. N. (2013). "Characterization and properties of recycled polypropylene/coconut shell powder composites: Effect of sodium dodecyl sulfate modification," *Polym-Plast. Technol. Eng.* 52(3), 287-294. DOI: 10.1080/03602559.2012.749282
- Demir, H., Atikler, U., Balkose, D., and Tihminlioglu, F. (2006). "The effect of fiber surface treatments on the tensile and water absorption properties of polypropylene-luffa fiber composites," *Compos. Part. A* 37(3), 447-456. DOI: 10.1016/j.compositesa.2005.05.036
- Eng, C. C., Ibrahim, N. A., Zainuddin, N., Ariffin, H., and Yunus, W. M. Z. W. (2014). "Compositional and morphological changes of chemical modified oil palm mesocarp fiber by alkaline bleaching and silane coupling agents," *BioResources* 9(3), 5290-5301. DOI: 10.15376/biores.9.3.5290-5301
- Faisal, Z. T., Amri, F., Salmah, H., and Tahir, I. (2010). "The effect of acetic acid on properties of coconut shell filled low density polyethylene composites," *Indo. J. Chem.* 10(3), 334-340. DOI: 10.14499/ijc-v10i3p334-340
- Fisher, T., Hajaligol, M., Waymack, B., and Kellogg, D. (2002). "Pyrolysis behavior and kinetics of biomass derived materials," *J. Analy. App. Pyrol.* 62(2), 331-349. DOI: 10.1016/S0165-2370(01)00129-2
- Ismail, H., Ahmad, Z., Nordin, R., and Rashid, A. R. (2009). "Processibility and miscibility studies of uncompatibilized linear low density polyethylene/poly(vinyl alcohol) blends," *Polym-Plast. Technol. Eng.* 48, 1191-1197. DOI: 10.1080/03602550903147379
- Ismail, H., Hamid Abdullah, A., and Abu Bakar, A. (2010). "Kenaf core reinforced high-density polyethylene/soya powder composites: The effects of filler loading and compatibilizer," *J. Reinf. Plast. Compos.* 29(16), 2489-2497. DOI: 10.1177/0731684409354392

- Maizatul, N., Norazowa, I., Yunus, W. M. Z. W., Khalina, A., and Khalisanni, K. (2013). "FTIR and TGA analysis of biodegradable poly(lactic acid)/treated kenaf bast fiber: Effect of plasticizers," *Pertanika. J. Sci. Technol.* 21(1), 151-160. ISSN: 0128-7680
- Majid, R. A., Ismail, H., and Taib, R. M. (2010). "Effect of polyethylene-g-maleic anhydride on properties of low density polyethylene/thermoplastic sago starch reinforced kenaf fiber composites," *Iran. Polym. J.* 19(7), 501-510.
- Malkapuram, R., Kumar, V., and Negi, Y. S. (2009). "Recent development in natural fiber reinforced polypropylene composites," *J. Reinf. Plast. Compos.* 28(10), 1169-1189. DOI: 10.1177/0731684407087759
- Meon, M. S., Othman, M. F., Husain, H., Remeli, M. F., and Syawal, M. S. M. (2012). "Improving tensile properties of kenaf fiber treated with sodium hydroxide," *Procedia. Eng.* 41, 1587-1592. DOI: 10.1016/j.proeng.2012.07.354
- Noranizan, A., and Ahmad, I. (2012). "Effect fo fiber loading and compatibilizer on rheological, mechanical and morphological behaviors," *J. Polym. Chem.* 2(2), 31-41. DOI: 10.4236/ojchem.2012.22005
- Nordin, R., Ismail, H., Ahmad, Z., and Rashid, A. (2012). "Performance improvement of (linear low-density polyethylene/poly(vinyl alcohol) blends by *in situ* silane crosslinking," *J. Vinyl. Add. Technol.* 18(2), 120-128. DOI: 10.1002/vnl.20294
- Nurfatimah, B., Chee, C. Y., Abdullah, L. C., Ratnam, C. T., and Azowa, N. (2014). "Effect of methyl methacrylate grafted kenaf on mechanical properties of polyvinyl chloride/ethylene vinyl acetate composites," *Compos Part A. Appl. Sci. Manuf.* 63, 45-50. DOI: 10.1016/j.compositesa.2014.03.023
- Osman, H., Ismail, H., and Mariatti, M. (2012). "Polypropylene/natural rubber composites filled with recycled newspaper: Effect of chemical treatment using maleic anhydride-grafted polypropylene and 3-aminopropyltriethoxysilane," *Polym. Compos.* 33(4), 609-618. DOI: 10.1002/pc.22178
- Pang, A. L., and Ismail, H. (2013). "Tensile properties, water uptake and thermal properties of polypropylene/waste pulverized tire/kenaf (PP/WPT/KNF) composites," *BioResources* 8(1), 806-817. DOI: 10.15376/biores.8.1.806-817
- Pang, A. L., and Ismail, H. (2014). "Studies on properties of polypropylene/waste tire dust/kenaf (PP/WTD/KNF) composites with addition of phthalic anhydride (PA) as a function of KNF loading," *J. Vinyl. Add. Technol.* 20(3), 193-200. DOI: 10.1002/vnl.21365
- Pang, A. L., Ismail, H., and Abu Bakar, A. (2015). "Effects of kenaf loading on processability and properties of linear low-density polyethylene/poly (vinyl alcohol)/kenaf composites," *BioResources* 10(4), 7302-7314. DOI: 10.15376/biores.10.4.7302-7314
- Pua, F.- L., Sapuan S. M., Zainudin, E. S., and Adibl, M. Z. (2013). "Effect of fiber surface modification on properties of kenaf/poly(vinyl alcohol) composites film," *J. Biobased Mater. Bioenergy* 7(1), 95-101. DOI: 10.1166/jbmb.2013.1270
- Rangel-Vazquez, N. A., and Leal-Garcia, T. (2010). "Spectroscopy analysis of chemical modification of cellulose fibers," *J. Mex. Chem. Soc.* 54(4), 192-197.
- Saba, N., Paridah, M. T., and Jawaid, M. (2015). "Mechanical properties of kenaf fiber reinforced polymer composites," *Construct. Build. Mater.* 76(2015), 87-96. DOI: 10.1016/j.conbuildmat.2014.11.043

- Sarifuddin, N., Ismail, H., and Ahmad, Z. (2013). "The effect of kenaf core fiber loading on properties of low density polyethylene/thermoplastic sago starch/kenaf core fiber composites," *J. Phys. Sci.* 24(2), 97-115.
- Tan, B. K., Ching, Y. C., Gan, S. N., Ramesh, S., and Rahman, M. R. (2014). "Water absorption properties of kenaf fibre-poly(vinyl alcohol) composites," *Mater. Res. Inno.* 18(S6), S6-144-S6-146. DOI: 10.1179/1432891714Z.000000000946

Article submitted: January 22, 2016; Peer review completed: April 9, 2016; Revisions accepted: May 8, 2016; Published: May 16, 2016.
DOI: 10.15376/biores.11.3.5889-5904